IMAGE RECONSTRUCTION BY ORTHOGONAL MOMENTS DERIVED BY THE PARITY OF POLYNOMIALS

*Bo Yang** *Wei Tang*† *Xiaofeng Chen*

School of Automation
Northwestern Polytechnical University
710072 Xi'an, China.

ABSTRACT

Moments are a kind of classical feature descriptors for image analysis. Orthogonal moments, due to their computation efficiency and numerical stability, have been widely developed. We propose a set of orthogonal polynomials which are derived from the parity of Hermite polynomials. The new orthogonal polynomials are composed of either odd orders or even ones of Hermite polynomials. They, however, are orthogonal in different domains. The corresponding orthogonal moments, Hermite-Fourier moments are defined. The computation strategy for these new moments is formulated in addition. Image reconstruction in comparison with Zernike moments as well as Fourier-Mellin moments shows the better image representation ability of the proposed moments.

***Index Terms*—** Orthogonal polynomials, Hermite-Fourier moments, image reconstruction, parity of polynomials, numerical integration

1. INTRODUCTION

Feature plays a fundamental role in image processing and computer vision. A variety of feature descriptors have been proposed so far, such as wavelet coefficients[1], moments, moment invariants [2], HOG[3], SIFT[4] etc.

As a kind of traditional and classical feature descriptors, moments are capable of extracting and representing the global feature of object with different degrees. Moreover, highlighted with efficient computation as well as low information redundancy, orthogonal moments are developed and introduced to various applications with respect to image processing.

Teague introduced invariant design and image reconstruction from Zernike Moments (ZMs)[5]. Pseudo-Zernike Moments (PZMs), that are similar to ZMs, were comparatively studied by recognizing handwritten numbers and aircrafts[6]. Fourier-Mellin Moments (FMMs), for more zeros in their radial polynomials, were developed and tested to have better image representation ability especially for small images[7]. Orthogonal moments, whose basis functions are composed of a radial orthogonal polynomial and a Fourier complex componential factor, were respectively developed from Chebyshev[8], Jacobi[9], Bessel[10] polynomials and exponent function[11].

Another type of orthogonal moments are those who are defined in a square or rectangular domain. Legendre moments are the most popular ones of this kind. There are a number of works related to computation and application of Legendre moments. The recent work is design of invariants from Legendre moments and their application to image watermark[12]. Shen proposed Gaussian-Hermite moments[13] and later Yang *et* al. performed image reconstruction and invariant design from such moments[14, 15]. Hosny tested image representation ability of Gegenbauer moments with a more accurate computation algorithm[16]. Orthogonal moments in discrete case were also proposed. Taking the discrete orthogonal polynomials as the basis functions is a general way to develop discrete orthogonal moments. This can be learned from Tchebichef[17], Krawtchouk[18], Hahn[19] and dual Hahn[20] moments.

We can learn from the works mentioned above that all orthogonal moments are defined by the existing orthogonal polynomials or functions. Although this way is quite reasonable and the most popular, it is not the only way to design orthogonal moments. Taking advantage of some properties of the existing orthogonal polynomials may generate new sets of orthogonal polynomials or functions, which may be probably used to develop new family of moments. In this paper we show how to use the parity of Hermite polynomials to generate new orthogonal bases. In addition, we define a new set of orthogonal moments called Hermite-Fourier Moments (HFMs) and demonstrate their image representation ability via image reconstruction.

The rest paper is organized as follows. Section 2 de-

*Thanks to the National Natural Science Foundation of China (Grant No. 61502389), by the Fundamental Research Funds for the Central Universities (Grant No. 3102018ZY025), by Fund Program for the Scientific Activity of Selected Returned Overseas Professionals in Shaanxi Province (Grant No. 2018024) and Science Foundation of Ministry of Education (Grant No. G2016001, X2017016).

†Thanks to the National Natural Science Foundation of China (Grant No. 61573289).

rives the new set of orthogonal bases from Hermite polynomials and defines the corresponding moments. Section 3 offers some techniques for accurate computation of the moments. Section 4 demonstrates the results of image reconstruction. Section 5 concludes the paper.

2. HERMITE-FOURIER MOMENTS

We use Hermite polynomials to derive new set of orthogonal bases. Hermite polynomial of order p is defined by

$$H_p(x) = (-1)^p \exp{(x^2)} \frac{d^p}{dx^p} \exp{(-x^2)}. \quad (1)$$

Hermite polynomials possess orthogonality because of

$$\int_{-\infty}^{\infty} H_p(x) H_q(x) \exp{(-x^2)} dx = \sqrt{\pi} 2^p p! \delta_{pq}, \quad (2)$$

where δ_{pq} represents the Kronecker symbol[21].

It is evident that Hermite polynomial is an even function when p is an even integer and an odd function when p is an odd one. We have the following conclusion derived from such parity property.

Theorem 1 *Let p and q be two non-negative integers. When p and q are **both even** numbers,*

$$\int_{0}^{\infty} H_p(x) H_q(x) \exp{(-x^2)} dx = \sqrt{\pi} 2^{p-1} p! \delta_{pq}. \quad (3)$$

*(3) is also established when p and q are **both odd** numbers.*

The proof of Theorem 1 is straightforward according to the parity of Hermite polynomials. This theorem is a chief contribution of the paper. It shows two facts. Firstly, the orthogonality domain is shrunk to $(0, \infty)$. Secondly, all Hermite polynomials of even (or odd) order form an independent orthogonality subset in this shrunk domain.

The orthogonality domain $(0, \infty)$ is facilitated to define radial polynomials or functions. By introducing a scale parameter σ to Gaussian envelop in (3), we define the p^{th} Radial Hermite Polynomial (RHP) as

$$\tilde{H}_p(r; \sigma) = \frac{1}{\sigma \sqrt{\sqrt{\pi} 2^{p-1} p!}} \left(\frac{\sigma}{r}\right)^{\frac{1}{2}} H_p\left(\frac{r}{\sigma}\right) \exp{(-\frac{r^2}{2\sigma^2})}. \quad (4)$$

Eq. (4) is not only orthogonal but also orthonormal, because

$$\begin{array}{c} \int_{0}^{\infty} \tilde{H}_p(r; \sigma) \tilde{H}_q(r; \sigma) r dr = \delta_{pq}, \\ (p, q) \in \{0, 2, \cdots\} \text{ or } (p, q) \in \{1, 3, \cdots\} \end{array}. \quad (5)$$

Fig. 1 shows the plotting of the first 5 RHPs of odd order and even order. The basis function of HFMs consists of a RHP and a Fourier complex componential factor

$$V_{pq}(r, \theta; \sigma) = \tilde{H}_p(r; \sigma) \exp{(iq\theta)}, \quad (6)$$

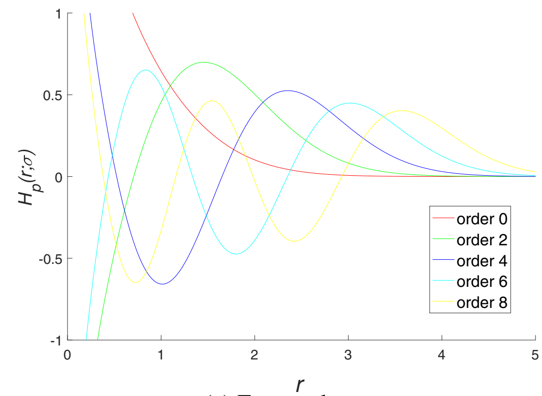

(a) Even order

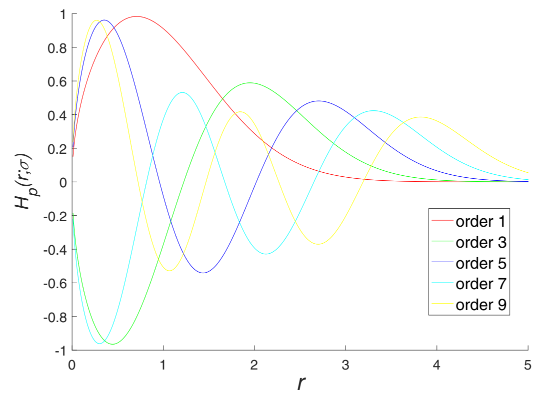

(b) Odd order

Fig. 1. Plotting of $\tilde{H}_p(r; \sigma)$ with $\sigma = 1.0$. Both RHPs of even order and odd one form independent orthogonality subsets, respectively.

with i is the imaginary unit. Note that (6) adopts polar coordinates (r, θ) instead of Cartesian coordinates (x, y). Consequently, for an image $f(r, \theta)$ its HFM of order p repetition q is formulated explicitly by

$$h_{pq} = \frac{1}{2\pi} \int_{0}^{2\pi} \int_{0}^{\infty} f(r, \theta) V^*_{pq}(r, \theta; \sigma) r dr d\theta, \quad (7)$$

where "*" denotes conjugate complex. Inversely, any image can be approximated by a set of HFMs within a maximum order P_{max}

$$\hat{f}_{P_{max}}(r, \theta) = \sum_{p=0}^{P_{max}} \sum_{q=-p}^{p} h_{pq} V_{pq}(r, \theta; \sigma). \quad (8)$$

3. COMPUTATION IN DISCRETE CASE

The orthogonality of RHPs is over $(0, \infty)$. It is not unit disc which is generally valid to the basis functions of ZMs, PZMs and FMMs. We can, however, transform it to unit disc for computation convenience. We take the outer unit disc for coordinate mapping in order to remove geometric error. Given a digital image $f(j,k)$ with size $N \times N$ pixels, coordinate transformation is implemented as follows,

$$\begin{cases} x_j = -\sqrt{2}/2 + \sqrt{2}(j-1)/(N-1) \\ y_k = -\sqrt{2}/2 + \sqrt{2}(k-1)/(N-1) \\ r_{j,k} = \sqrt{x_j^2 + y_k^2}/\sigma \\ \theta_{j,k} = \mathrm{actan}(y_k/x_j) \end{cases}, \ (j,k) = 1,2,\cdots N \,. \tag{9}$$

Another kind of computation error, numerical integration error is reduced by the following approximation operation,

$$h_{pq} = \frac{1}{2\pi}\sum_{j=1}^{N}\sum_{k=1}^{N} f(x_j, y_k)\Psi_{pq}(j,k), \quad x_j^2 + y_k^2 \le 1 \tag{10}$$

where

$$\Psi_{pq}(j,k) = \int_{a_j}^{a_{j+1}} \int_{b_k}^{b_{k+1}} V_{pq}^*(x,y;\sigma)dxdy. \tag{11}$$

(11) can be more accurately computed via Gauss-Legendre numerical integration[22], which is further decomposed

$$\Psi_{pq}(j,k) = \frac{(a_{j+1}-a_j)(b_{k+1}-b_k)}{4} \times \sum_{u=1}^{M}\sum_{v=1}^{M} \omega_u \omega_v V_{pq}^*(x_u, y_v;\sigma). \tag{12}$$

In (12) M is number of sampling point, x_u denotes Gaussian sampling point and ω_u represents its weight. The same meanings are to y_v and ω_v. The integration interval generated by any pixel is computed below

$$\begin{cases} a_j = x_{j+1} - 1/(\sqrt{2}(N-1)), \ j = 0,1,\cdots N-1 \\ a_j = x_j + 1/(\sqrt{2}(N-1)), \ j = N \end{cases}. \tag{13}$$

When performing image reconstruction, (8) should use a dynamic σ to generate a more precise reconstructed image. In this paper we adopt σ selection recommended in [23], which is

$$\sigma_{p_{max}} = 0.90 \cdot p_{max}^{-0.52}, \tag{14}$$

here p_{max} represents the maximum order that is used to reconstruct the image.

4. EXPERIMENTS

Three experiments were carried out to test the effectiveness of computation implementation and the performance of HFMs. The error is defined by

$$e_p = \frac{\sum_{j=1}^{N}\sum_{k=1}^{N}\left(f(j,k) - \hat{f}_p(j,k)\right)^2}{\sum_{j=1}^{N}\sum_{k=1}^{N} f(j,k)^2}. \tag{15}$$

The first one is to demonstrate the improvement in reconstructed image brought by the algorithm in Section 3. We reconstructed popular gray image “lena” (256×256 pixels) from HFMs by the proposed computation method and Zeroth-Order Approximation (ZOA) algorithm. Fig. 2 shows the reconstruction by odd-order HFMs from order 1 up to 79. When high order moments are involved in, the reconstructed images are quite different. ZOA produces sharp numerical error in the centers and around the corners of reconstructed images. However, the proposed computation algorithm can reduce such error and produce more accurate reconstructed images.

The second one is to evaluate image representation ability of HFMs via reconstruction. ZMs and FMMs were also employed to reconstruct for comparison. Gray image “baboon” (256×256 pixels) was selected as the reference. ZMs was implemented by Kintner’s method in[24] and FMs was computed by the way in[22]. The results are shown in Fig. 3, from which we can see image reconstruction by three classes of moments of the first 75 orders. HFMs give the best reconstruction in comparison with the other two kinds of orthogonal moments.

The last experiment is to test noise robustness. Gray image “goldhill” (256×256 pixels) was added Gaussian White Noise (GWN) and Salt and Pepper Noise (SPN), respectively (see Fig. 4(a) and (b)). Reconstructing these noisy images and then comparing the reconstructions with the noise-free one was conducted with HFMs and FMMs. The results were illustrated in Fig. 4. It can be learned from the figure that with the order growing up, the reconstructed images have ever-decreasing error until the order reaches a certain number. This means that the moments whose orders are higher than the number are strongly influenced by the noise. This also conforms to the fact that high order moments are more sensitive to noise. However, HFMs give the better reconstructions in two noisy cases than FMMs do.

(a) ZOA method (b) Proposed computation

Fig. 2. Reconstruction of image “lena” by HFMs of odd order up to order 79 ($1, 3, \cdots, 79$ total 40 different orders). (a) by ZOA with $e = 0.0257$. (b) by the proposed computation algorithm with $e = 0.0141$.

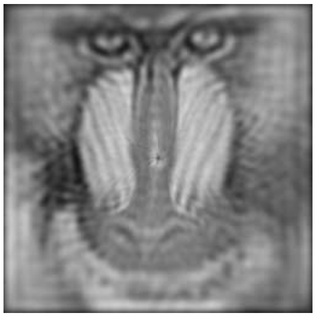

(a) by HFMs of first 31 orders

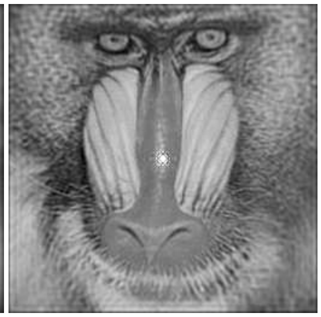

(b) by HFMs of first 75 orders

(c) by ZMs of first 31 orders

(d) by ZMs of first 75 orders

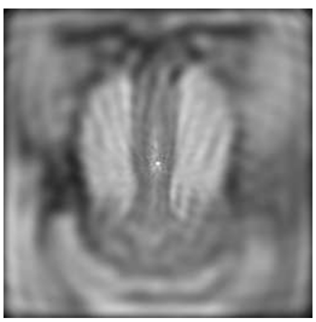

(e) by FMMs of first 31 orders

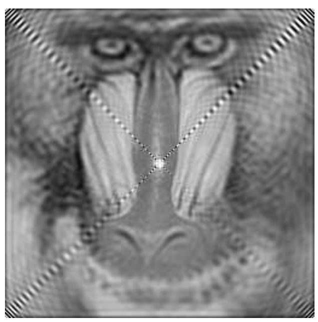

(f) by FMMs of first 75 orders

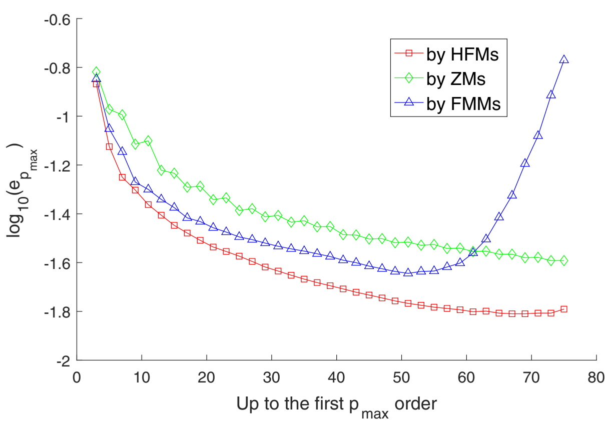

(g) Reconstruction vs. order

Fig. 3. Reconstruction by different moments.

(a) with GWN

(b) with SPN

(c) by first 51 HFMs in GWN

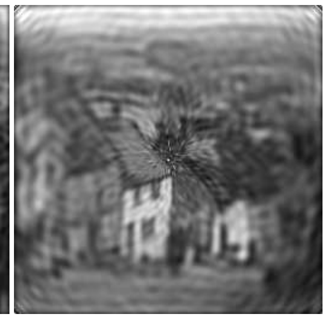

(d) by first 51 FMMs in SPN

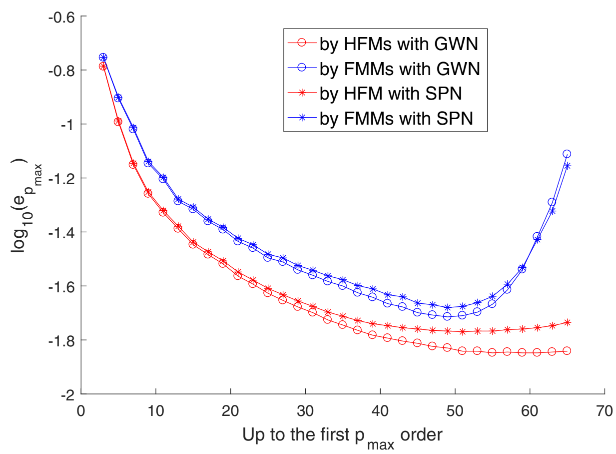

(e) Reconstruction vs. order

Fig. 4. Noisy image reconstruction by different moments.

5. CONCLUSION

We propose a new set of orthogonal moments called HFMs in this paper. Their basis function is composed of a radial polynomial derived from the parity of Hermite polynomial and a Fourier complex componential factor. Image reconstruction from HFMs is investigated. The experiments show the effectiveness of computation algorithm and the superior image representation ability of HFMs.

6. REFERENCES

[1] M.N. Do and M. Vetterli, "Wavelet-based texture retrieval using generalized Gaussian density and Kullback-Leibler distance," *IEEE Transactions on Image Processing*, vol. 11, no. 2, pp. 146–158, Feb. 2002.

[2] J. Flusser, T. Suk, and B. Zitová, *2D and 3D Image Analysis by Moments*, Wiley, Chichester, U.K., 2016.

[3] N. Dalal and B. Triggs, "Histograms of oriented gradients for human detection," in *Proc. of IEEE Computer Society Conference on Computer Vision and Pattern Recognition*, San Diego, USA, July 2005.

[4] D. Lowe, "Distinctive image features from scale-invariant keypoints," *International Journal of Computer Vision*, vol. 60, no. 2, pp. 91–110, Nov. 2004.

[5] M. R. Teague, "Image analysis via general theory of moments," *Journal of the Optical Society of America*, vol. 70, no. 8, pp. 920–930, Aug. 1980.

[6] S. O. Belkasim, M. Shridhar, and M. Ahmadi, "Pattern recognition with moment invariants: A comparative study and new results," *Pattern Recognition*, vol. 24, no. 12, pp. 1117–1138, May 1991.

[7] Y.L. Sheng and L.X. Shen, "Orthogonal Fourier-Mellin moments for invariant pattern recognition," *Journal of the Optical Society of America A*, vol. 11, no. 6, pp. 1748–1757, June 1994.

[8] Z.L. Ping, R.G. Wu, and Y.L. Sheng, "Image description with Chebyshev-Fourier moments," *Journal of the Optical Society of America A*, vol. 19, no. 9, pp. 1748–1754, Sept. 2002.

[9] Z.L. Ping, H.P. Ren, J. Zou, Y.L. Sheng, and W. Bo, "Generic orthogonal moments: Jacobi-Fourier moments for invariant image description," *Pattern Recognition*, vol. 40, no. 4, pp. 1245–1254, Apr. 2007.

[10] B. Xiao, J.F. Ma, and X. Wang, "Image analysis by Bessel−Fourier moments," *Pattern Recognition*, vol. 43, no. 8, pp. 2620–2629, Aug. 2010.

[11] H.T. Hu, Y.D. Zhang, C. Shao, and Q. Ju, "Orthogonal moments based on exponent functions: Exponent-Fourier moments," *Pattern Recognition*, vol. 47, no. 8, pp. 2596–2606, Aug. 2014.

[12] H. Zhang, H. Z. Shu, G. Coatrieux, J. Zhu, Q. M. Jonathan Wu, Y. Zhang, H. Q. Zhu, and L. M. Luo, "Affine Legendre moment invariants for image watermarking robust to geometric distortions," *IEEE Transactions on Image Processing*, vol. 20, no. 8, pp. 2189–2199, Feb. 2011.

[13] J. Shen, "Orthogonal Gaussian-Hermite moments for image characterization," in *Proc. SPIE on Intelligent Robots and Computer Vision*, Pittsburgh, USA, Oct. 1997, pp. 224–233.

[14] B. Yang and M. Dai, "Image reconstruction from continuous Gaussian-Hermite moments implemented by discrete algorithm," *Pattern Recognition*, vol. 45, no. 4, pp. 1602–1616, Apr. 2012.

[15] B. Yang, J. Kostkova, J. Flusser, and T. Suk, "Rotation invariants of vector fields from orthogonal moments," *Pattern Recognition*, vol. 74, pp. 110–121, Feb. 2018.

[16] K.M. Hosny, "Image representation using accurate orthogonal Gegenbauer moments," *Pattern Recognition Letters*, vol. 32, no. 6, pp. 795–804, Apr. 2011.

[17] R. Mukundan, S.H. Ong, and P.A. Lee, "Image analysis by Tchebichef moments," *IEEE Transactions on Image Processing*, vol. 10, no. 9, pp. 1357–1364, Sept. 2001.

[18] P. Yap, R. Paramesran, and S. Ong, "Image analysis by Krawtchouk moments," *IEEE Transactions on Image Processing*, vol. 12, no. 11, pp. 1367–1377, Oct. 2003.

[19] P.T. Yap, R. Paramesran, and S.H. Ong, "Image analysis using Hahn moments," *IEEE Transactions on Pattern Analysis and Machine Intelligence*, vol. 29, no. 11, pp. 2057–2062, Sept. 2007.

[20] H.Q. Zhu, H.Z. Shu, J. Zhou, L.M. Luo, and J.L. Coatrieux, "Image analysis by discrete orthogonal dual Hahn moments," *Pattern Recognition Letters*, vol. 28, no. 13, pp. 1688–1704, Oct. 2007.

[21] S. Gabor, *Orthogonal polynomials*, American Mathematical Society, Providence, Rhode Island, U.S.A, 1967.

[22] C. Singh and R. Upneja, "Accurate computation of orthogonal Fourier-Mellin moments," *Journal of Mathematical Imaging and Vision*, vol. 44, no. 3, pp. 411–431, Nov. 2012.

[23] B. Yang and M. Dai, "Image analysis by Gaussian-Hermite moments," *Signal Processing*, vol. 91, no. 10, pp. 2290–2303, Oct. 2011.

[24] C.W. Chong, P. Raveendran, and R. Mukundan, "A comparative analysis of algorithms for fast computation of Zernike moments," *Pattern Recognition*, vol. 36, no. 3, pp. 731–742, Mar. 2003.